Journal of Superconductivity and Novel Magnetism (2018) 31:3711–3716
https://doi.org/10.1007/s10948-018-4641-8

ORIGINAL PAPER

Magnetic Transition and Magnetocaloric Effect of $Gd_{1-x}Nd_xMn_2Ge_2$ ($x = 0.3$ and 0.4) Compounds

J. Wang[1] · D. L. Guo[1] · S. D. Lin[1] · B. Wen[1] · M. H. Rong[1] · G. H. Rao[1] · H. Y. Zhou[1]

Received: 17 February 2018 / Accepted: 7 March 2018 / Published online: 17 March 2018

Abstract
$Gd_{1-x}Nd_xMn_2Ge_2$ compounds with $x = 0.3$ and 0.4 were prepared by arc melting and crystallized in the $ThCr_2Si_2$-type structure with the space group I4/mmm based on X-ray powder diffraction (XRD) results. Magnetic transition and magnetocaloric effect (MCE) of the $Gd_{1-x}Nd_xMn_2Ge_2$ compounds were investigated by magnetic measurements on a physical property measurement system (PPMS). $Gd_{0.7}Nd_{0.3}Mn_2Ge_2$ compound exhibits complicated magnetic transitions at around 63 K (T_{comp}), 86 K (T_1), 136 K (T_C), 260 K (T_N^{inter}), and 347 K (T_C^{inter}), respectively, while $Gd_{0.6}Nd_{0.4}Mn_2Ge_2$ compound shows a spin re-orientation transition at about 52 K. Combined with isothermal magnetization curves and the Maxwell relation, the maximum magnetic entropy changes of $Gd_{0.7}Nd_{0.3}Mn_2Ge_2$ and $Gd_{0.6}Nd_{0.4}Mn_2Ge_2$ were calculated to be 4.31 and 5.15 J kg^{-1} K^{-1} under the applied magnetic field changing from 0 to 5 T, respectively.

Keywords $Gd_{1-x}Nd_xMn_2Ge_2$ compounds · Magnetic transition · Magnetocaloric effect

1 Introduction

Ternary intermetallic compounds containing rare earth (RE) elements, transition metals, and third element Ge and/or Si (e.g., $REMn_2Ge_2$ and $REMn_2Si_2$) have been studied extensively due to their interesting physical properties [1–8]. $REMn_2Ge_2$ compounds with the body-centered tetragonal $ThCr_2Si_2$-type structure manifest complex magnetic transitions due to the interplay between 3d and 4f magnetism and the strong dependence of the magnitude of the Mn moment and the magnetic state of the Mn sublattice on the Mn–Mn interatomic distance [9–11]. Magnetic transitions and magnetic properties of $REMn_2Ge_2$ compounds are strongly dependent on the Mn–Mn intraplanar and interplanar exchange interactions, which affects the Mn–Mn interatomic distance in the ab plane ($d^a_{Mn\text{-}Mn}$) governed by the lattice parameter (a) [12–23]. The critical distance of $d^a_{Mn\text{-}Mn}$ and lattice parameter (a) is 2.870 and 4.060 Å, respectively, based on the reported experimental results [12–21]. If $d^a_{Mn\text{-}Mn} > 2.870$ Å ($a > 4.060$ Å), the intralayer (in-plane) Mn–Mn coupling is antiferromagnetic, while the interlayer (along the c-axis) Mn–Mn coupling is ferromagnetic. In the case of 2.840 Å $< d^a_{Mn\text{-}Mn} <$ 2.870 Å (4.020 Å $< a <$ 4.060 Å), the intralayer and interlayer Mn–Mn couplings are antiferromagnetic. When $d^a_{Mn\text{-}Mn} <$ 2.840 Å ($a <$ 4.020 Å), there is no intralayer in-plane spin component and the interlayer Mn–Mn coupling is collinear ferromagnetic or antiferromagnetic along the c-axis [13–21].

Among these $REMn_2Ge_2$ compounds, magnetic transitions of $Nd_{1-x}Y_xMn_2Ge_2$ [24], $Nd_{1-x}Er_xMn_2Ge_2$ [25], $Gd_{0.925}La_{0.075}Mn_2Ge_2$ [26], and $Nd_{1-x}Gd_xMn_2Ge_2$ [27] compounds were investigated experimentally. $Nd_{1-x}Gd_xMn_2Ge_2$ ($x \leq 0.6$) compounds show the ferromagnetic transition with a spin re-orientation at low temperature, while $Nd_{1-x}Gd_xMn_2Ge_2$ ($0.7 \leq x < 1$) compounds exhibit the ferromagnetic behavior with the compensation point and re-entrant ferrimagnetism [27]. In addition, magnetocaloric effect (MCE) of $REMn_2Ge_2$ compounds, e.g., $Gd_{1-x}Sm_xMn_2Ge_2$ [28], $Pr_{1-x}Y_xMn_2Ge_2$ [29], $Nd(Mn_{1-x}Fe_x)_2Ge_2$ [30], and $Nd_{0.2}Gd_{0.8}Mn_2Ge_2$ [31], were studied experimentally. The maximum magnetic entropy change of $Gd_{0.8}Nd_{0.2}Mn_2Ge_2$ under a magnetic

✉ J. Wang
wangjiang158@163.com

✉ M. H. Rong
rongmh124@guet.edu.cn

[1] School of Materials Science and Engineering and Guangxi Key Laboratory of Information Materials, Guilin University of Electronic Technology, Guilin 541004, China

field change of 1 T was negative (-0.812 J kg^{-1} K^{-1}) at the re-entrant ferromagnetic transition temperature, while it was positive (0.682 J kg^{-1} K^{-1}) at the antiferro-ferromagnetic transition temperature [31].

In order to better understand the effect of substitution of Nd for Gd on magnetic properties of $GdMn_2Ge_2$ compound, the crystal structure, magnetic transitions, and magnetocaloric properties of $Gd_{1-x}Nd_xMn_2Ge_2$ ($x = 0.3$ and 0.4) compounds were investigated experimentally in this work.

2 Experiment

$Gd_{1-x}Nd_xMn_2Ge_2$ ($x = 0.3$ and 0.4) compounds were prepared in an arc furnace by arc-melting pure elements (99.99% purity) using a non-consumable tungsten electrode under an inert argon atmosphere. To compensate the weight loss during the melting and annealing procedure, 3% excess of Mn was added. Ingots with the mass of about 3 g were melted four times to achieve good homogeneity. The ingots were annealed in an evacuated quartz tube at 1173 K for 240 h and then quenched in ice water.

The crystal structure and phase identification of the samples were determined by X-ray powder diffraction (XRD, PLXcel 3D) using Cu Kα radiation in the range from 20° to 120° with 0.2626 step sizes at 45 kV and 40 mA at room temperature. The crystal structure was refined by the Rietveld technique using the GSAS software. Magnetization measurements were carried out using a physical property measurement system (PPMS-9, Quantum Design) in the temperature range of 10 ∼ 380 K under applying magnetic field of 200 Oe. The temperature dependence of magnetization was recorded following zero-field-cooled (ZFC) and field-cooled (FC) measurement protocols. The samples were cooled in the absence of a field (ZFC) or in the presence of a field (FC), and then the magnetization was measured during warming. Isothermal magnetization of the samples was measured by PPMS at different temperatures under the applied magnetic field of up to 5 T.

3 Results and Discussion

3.1 Phase Analysis

Figure 1 is the Rietveld refinement results of the XRD patterns of $Gd_{1-x}Nd_xMn_2Ge_2$ ($x = 0.3$ and 0.4) compounds at room temperature. The refinement results confirm that the compounds are single phase crystallizing in the $ThCr_2Si_2$-type structure with the space group I4/mmm. The lattice parameters of $Gd_{0.7}Nd_{0.3}Mn_2Ge_2$ and $Gd_{0.6}Nd_{0.4}Mn_2Ge_2$ derived from the Rietveld refinements

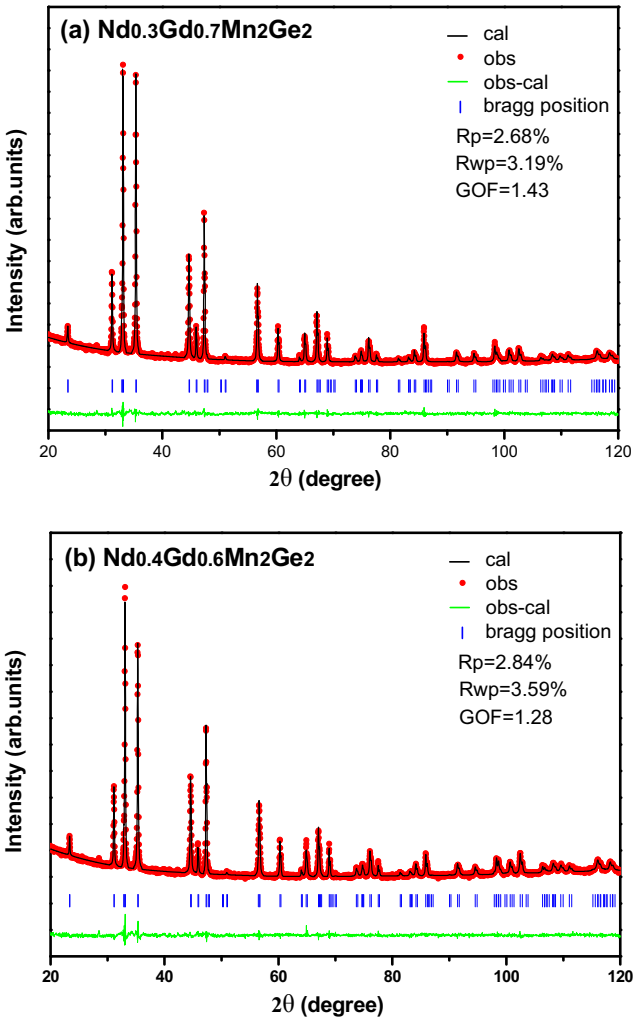

Fig. 1 The Rietveld refinement results of XRD patterns of **a** $Gd_{0.7}Nd_{0.3}Mn_2Ge_2$ and **b** $Gd_{0.6}Nd_{0.4}Mn_2Ge_2$. The red points and the solid lines are the experimental and calculated XRD patterns, respectively. The green lines are the differences between the experimental and calculated intensities, while the vertical bars indicate the position of Bragg refractions

are $a = 4.055(6)$ Å, $c = 10.890(7)$ Å and $a = 4.060(6)$ Å, $c = 10.893(8)$ Å, respectively, which are consistent with the reported data ($a = 4.054$ Å, $c = 10.884$ Å and $a = 4.061$ Å, $c = 10.888$ Å) [27].

3.2 Magnetic Transitions

Figure 2 shows the temperature dependence of magnetization of $Gd_{1-x}Nd_xMn_2Ge_2$ ($x = 0.3$ and 0.4) compounds in the temperature range of 10–380 K in a magnetic field of 200 Oe. In Fig. 2a, $Gd_{0.7}Nd_{0.3}Mn_2Ge_2$ compound exhibits a re-entrant ferromagnetism accompanied with a sequence of magnetic transitions from antiferromagnetic to ferromagnetic, antiferromagnetic, and ferromagnetic states according to the experimental results [32, 33], which is similar with the

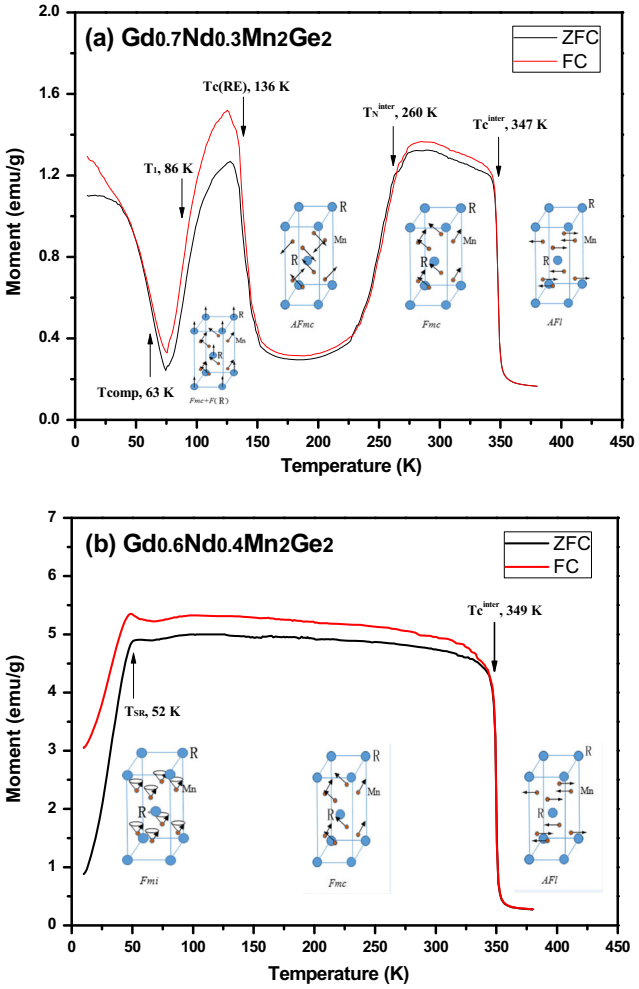

Fig. 2 Temperature dependence of magnetization of **a** $Gd_{0.7}Nd_{0.3}Mn_2Ge_2$ and **b** $Gd_{0.6}Nd_{0.4}Mn_2Ge_2$ measured in the applied magnetic field of 200 Oe

magnetic behavior of $SmMn_2Ge_2$ [34]. A transition occurs from the intralayer antiferromagnetic (AFl) state to the canted ferromagnetic (Fmc) state at 347 K (T_C^{inter}). T_C^{inter} corresponds to the minimum of dM/dT of the FC curve. With decreasing temperature, a transition from canted ferromagnetic (Fmc) state to an interlayer antiferromagnetic (AFmc) state at 260 K (T_N^{inter}) is found. T_N^{inter} corresponds to the maximum of dM/dT of the FC curve. The AFmc state is stable until about 136 K (T_C(RE)). It shows a re-entrant ferromagnetism below T_C(RE) because of the long-range ordering of Gd moment coupling ferromagnetically with ferromagnetic component of the Mn sublattice. At the lower temperature, the compensation temperature (T_{comp}) was found at 63 K. The magnetic moment of the RE sublattice increased more rapidly with the decreasing temperature than that of the Mn sublattice, yielding the compensation point at 63 K. On the other hand, in Fig. 2b, the ZFC and FC magnetizations of $Gd_{0.6}Nd_{0.4}Mn_2Ge_2$ compound show two magnetic transitions temperatures (T_{SR} and T_C^{inter}). According to the experimental results [27], the spin re-orientation behavior is observed below T_C^{inter}. The spin re-orientation temperature (T_{SR}) was determined to be 52 K by the cusp maximum of the magnetization FC curve, which corresponds to a re-arrangement of the Mn order from a canted ferromagnetic structure (Fmc) to a conical ferromagnetic structure (Fmi) with the ferromagnetic order perpendicular to the tetragonal c-axis, resulting in a stronger ferromagnetic component.

As can be seen in Fig. 2, $Gd_{0.7}Nd_{0.3}Mn_2Ge_2$ compound exhibits multiple magnetic transitions in the temperature range of 10–380 K, while $Gd_{0.6}Nd_{0.4}Mn_2Ge_2$ compound has two magnetic transitions in the same temperature region. Since the atomic radius of Nd is larger than that of Gd, the substitution of Nd for Gd results in an increase of the Mn–Mn bond lengths. The $d^a_{Mn\text{-}Mn}$ (2.8677 Å) of $Gd_{0.7}Nd_{0.3}Mn_2Ge_2$ compound is slightly less than the critical distance (2.870 Å). The interlayer and intralayer Mn–Mn exchange couplings in $Gd_{0.7}Nd_{0.3}Mn_2Ge_2$ compound are antiferromagnetic, which leads to the formation of the AFmc-type antiferromagnetic structure below T_N^{inter} [12–20]. Meanwhile, the $d^a_{Mn\text{-}Mn}$ (2.8713 Å) of $Gd_{0.6}Nd_{0.4}Mn_2Ge_2$ compound is slightly larger than the critical distance (2.870 Å). The interlayer Mn–Mn exchange coupling in $Gd_{0.6}Nd_{0.4}Mn_2Ge_2$ compound is ferromagnetic, and the intralayer Mn–Mn exchange coupling is antiferromagnetic, resulting in the formation of the canted Fmc-type ferromagnetic structure [12–20]. It confirms that the interlayer and intralayer Mn–Mn exchange interactions are very sensitive to the intralayer distance ($d^a_{Mn\text{-}Mn}$), resulting in the ferromagnetic or antiferromagnetic ordering of the Mn–Mn coupling.

In addition, the ZFC and FC curves of $Gd_{0.6}Nd_{0.4}Mn_2Ge_2$ compound split below T_C^{inter} in Fig. 2b. During the FC process, the ferromagnetic component of Mn moment has a preferred orientation in an external field [32, 34], while that is pinned randomly during ZFC process and therefore the overall magnetization of the compound in the ZFC curve is smaller than that in the FC curve [33, 34]. It is worth noting that both the FC and ZFC magnetizations tend to have very low values below T_{SR}.

3.3 Magnetocaloric Effect

Figure 3 shows the isothermal magnetization of $Gd_{1-x}Nd_xMn_2Ge_2$ ($x = 0.3$ and 0.4) compounds measured in the vicinity of the transition temperature (T_C^{inter}) with the magnetic field change from 0 to 5 T. As manifested in Fig. 3a, the magnetization of $Gd_{0.7}Nd_{0.3}Mn_2Ge_2$ compound increases rapidly under low fields and slowly under the high fields below T_C^{inter}, indicating the possibility of some antiferromagnetic components in this temperature

range, whereas the magnetization of the compound shows antiferromagnetic behavior at high temperature (above T_C^{inter}). In Fig. 3b, $Gd_{0.6}Nd_{0.4}Mn_2Ge_2$ compound has the ferromagnetic behavior at low temperature (below T_C^{inter}), while it shows antiferromagnetic behavior at high temperature (above T_C^{inter}). Moreover, the magnetization of $Gd_{0.6}Nd_{0.4}Mn_2Ge_2$ compound increases more rapidly at low magnetic field than that of $Gd_{0.7}Nd_{0.3}Mn_2Ge_2$ compound and shows a tendency to approach the saturation with increasing applied magnetic field.

In general, Arrott plots are used to determine the type of the phase transition of a compound near T_C^{inter} according to the Inoue-Shimizu model [35]. This model involves a Landau expansion of the magnetic free energy (F) of up to the sixth power of the total magnetization (M).

$$F = \frac{C_1(T)}{2}M^2 + \frac{C_3(T)}{4}M^4 + \frac{C_5(T)}{6}M^6 - \mu_0 MH \quad (1)$$

It has been pointed out that the order of a transition is closely related to the sign of the Landau coefficient $C_3(T)$ at the Curie temperature [36]. The transition is of the first order if $C_3(T_C)$ is negative, while it is of the second order for positive $C_3(T_C)$. The sign of $C_3(T_C)$ could be determined by means of Arrott plots [37]. If the Arrott plot is S-shape near the transition temperature, $C_3(T_C)$ is negative, otherwise it is positive. Figure 4 is the Arrott plots of $Gd_{1-x}Nd_xMn_2Ge_2$ ($x = 0.3$ and 0.4) compounds at different temperatures. As shown in Fig. 4a, b, no S-shaped curve is shown near T_C^{inter}. Therefore, the magnetic transition of $Gd_{1-x}Nd_xMn_2Ge_2$ ($x = 0.3$ and 0.4) compounds at 347 and 349 K (T_C^{inter}) is a second-order transition.

The magnetic entropy change (ΔS) was calculated using Maxwell's thermodynamic relation, $\left(\frac{\partial S}{\partial H}\right)T = \left(\frac{\partial M}{\partial T}\right)H$. The magnetic entropy change is given by:

$$\Delta S(T, H) = S(T, H) - S(T, 0) = -\int_0^H \left(\frac{\partial M}{\partial T}\right) dH \quad (2)$$

where ΔS, M, H, and T are the magnetic entropy change, magnetization, applied magnetic field, and the temperature

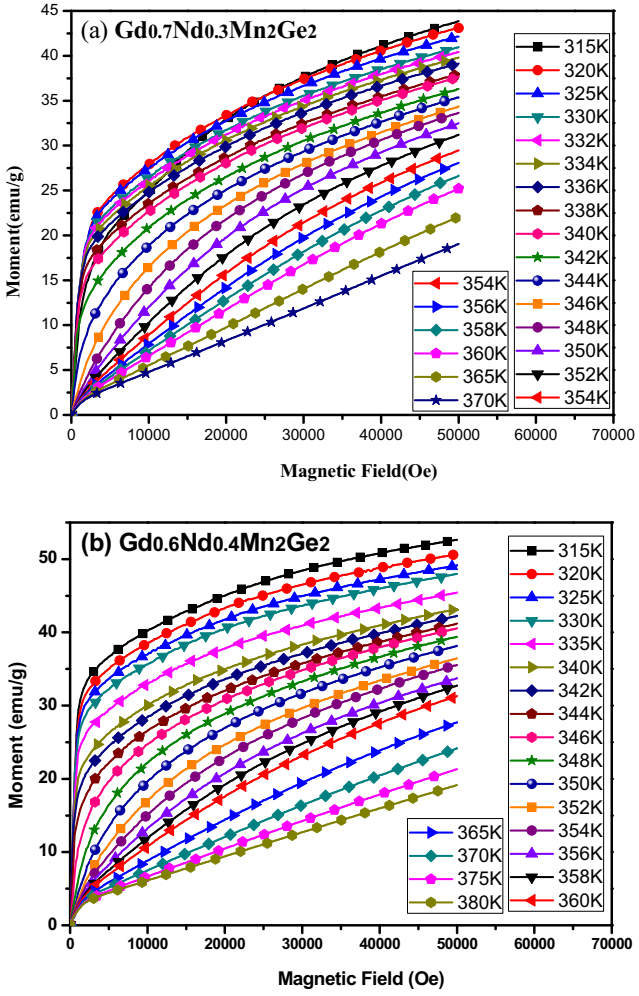

Fig. 3 Isothermal magnetization curves of **a** $Gd_{0.7}Nd_{0.3}Mn_2Ge_2$ and **b** $Gd_{0.6}Nd_{0.4}Mn_2Ge_2$ measured at different temperatures close to T_C^{inter}

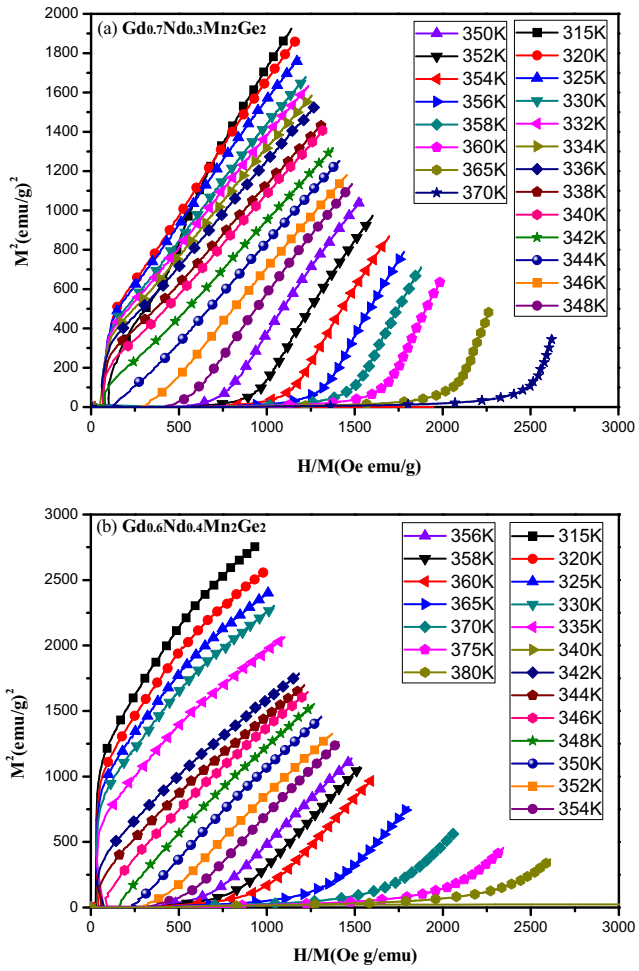

Fig. 4 Arrott plots of **a** $Gd_{0.7}Nd_{0.3}Mn_2Ge_2$ and **b** $Gd_{0.6}Nd_{0.4}Mn_2Ge_2$ at different temperatures close to T_C^{inter}(Mn)

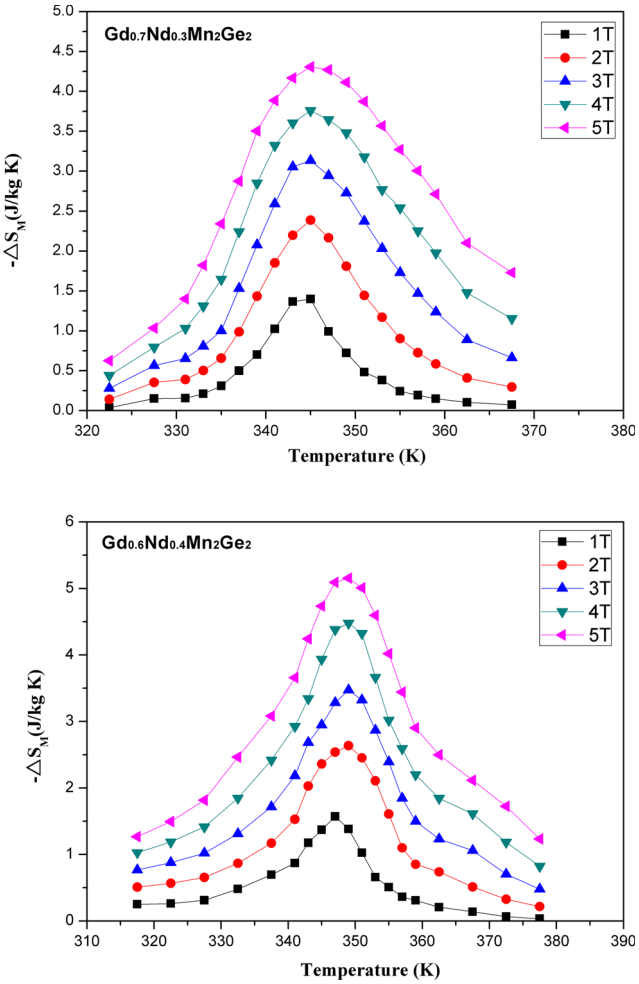

Fig. 5 Temperature dependence of magnetic entropy changes of **a** $Gd_{0.7}Nd_{0.3}Mn_2Ge_2$ and **b** $Gd_{0.6}Nd_{0.4}Mn_2Ge_2$ under different applied magnetic fields

of the system, respectively. Equation (2) can be approximated by the following expression [38]:

$$\Delta S = -\sum_i \frac{1}{T_{i+1} - T_i}(M_{i+1} - M_i)_H \Delta H_i \quad (3)$$

where M_i and M_{i+1} are the magnetization values measured in a field H at the temperatures T_i and T_{i+1}, respectively.

Using equation (3) and the isothermal magnetization curves, the temperature dependence of the magnetic entropy change were derived for $Gd_{0.7}Nd_{0.3}Mn_2Ge_2$ and $Gd_{0.6}Nd_{0.4}Mn_2Ge_2$ compounds (seen in Fig. 5). As can be seen, the magnetic ΔS increases gradually near the transition temperature. In this work, the maximum magnetic ΔS of $Gd_{1-x}Nd_xMn_2Ge_2$ ($x = 0.3$ and 0.4) compounds for a magnetic field change of 5 T close to the transition temperature T_C^{inter}(Mn) were calculated to be 4.31 and 5.15 J kg^{-1} K^{-1}, respectively. Under the similar magnetic transition temperature range and same applied magnetic field change, the maximum values of the magnetic ΔS are 2.35 and 1.84 J kg^{-1} K^{-1} for $Nd(Mn_{1-x}Fe_x)_2Ge_2$ ($x = 0.1$ and 0.2) [30], −1.0 and −1.1 J kg^{-1} K^{-1} for $Gd_{1-x}Sm_xMn_2Ge_2$ ($x = 0.4$ and 0.6) [28], and 2.94 and 3.47 J kg^{-1} K^{-1} for $Pr_{1-x}Y_xMn_2Ge_2$ ($x = 0.2$ and 0.5) [29].

4 Conclusions

In this work, the crystal structure, magnetic transitions, and magnetocaloric properties of the $Gd_{1-x}Nd_xMn_2Ge_2$ ($x = 0.3$ and 0.4) compounds were investigated experimentally by XRD and magnetic measurements. The following conclusions were drawn:

(1) XRD results confirm that the crystal structure of Gd_{1-x} $Nd_xMn_2Ge_2$ ($x = 0.3$ and 0.4) compounds is the $ThCr_2Si_2$-type structure with the space group I4/mmm. The Rietveld refinement results show that the lattice parameters of these two compounds are well consistent with the reported experimental data.

(2) The magnetization measurements reveal that $Gd_{0.7}$ $Nd_{0.3}Mn_2Ge_2$ compound shows complex magnetic states with multiple magnetic transitions, including AFl-type antiferromagnetism, Fmc-type canted ferromagnetism, AFmc-type antiferromagnetism, and the re-entrant ferrimagnetism, while $Gd_{0.6}Nd_{0.4}Mn_2Ge_2$ compound exhibits a spin re-orientation transition with the AFl-type antiferromagnetism and the Fmc-type canted ferromagnetism.

(3) Using the Maxwell relation, magnetic entropy changes of $Gd_{1-x}Nd_xMn_2Ge_2$ ($x = 0.3$ and 0.4) compounds are calculated from isothermal magnetization curves measured at different temperatures. Under the magnetic field change of 5 T, the maximum magnetic entropy changes of $Gd_{0.7}Nd_{0.3}Mn_2Ge_2$ and $Gd_{0.6}Nd_{0.4}Mn_2$ Ge_2 compounds are 4.31 and 5.15 J kg^{-1} K^{-1}, respectively.

Funding Information This work was supported financially by the National Natural Science Foundation of China (51461013, 51761008), National Basic Foundation of China (973 Program, 2014CB643703), Guangxi Natural Science Foundation (2016GXNSFDA380015, 2016GXNSFGA380001), and Innovation Project of GUET Graduate Education (2016YJCX25).

References

1. Kolmakova, N.P., Sidorenko, A.A., Levitin, R.Z.: Low Temp. Phys. **28**, 653 (2002)
2. Mukherjee, K., Iyer, K.K., Sampathkumaran, E.V.: EPL **90**, 17007 (2010)
3. Kervan, N., Kiliç, A., Kervan, S., Gencer, A.: Solid State Commun. **138**, 55 (2006)

4. Li, L., Saensunon, B., Hutchison, W.D., Huo, D., Nishimura, K.: J. Alloy. Compd. **582**, 670 (2014)
5. Li, L., Nishimura, K., Hutchison, W.D., Qian, Z., Huo, D., Namiki, T.: Appl. Phys. Lett. **100**, 152403 (2012)
6. Wang, J.L., Campbell, S.J., Cadogan, J.M., Studer, A.J., Zeng, R., Dou, S.X.: Appl. Phys. Lett. **98**, 232509 (2011)
7. Mushnikov, N.V., Gerasimov, E.G., Terentev, P.B., Gaviko, V.S., Yazovskikh, K.A., Aliev, A.M.: J. Magn. Magn. Mater. **89**, 440 (2017)
8. Wang, J.L., Caron, L., Campbell, S.J., Kennedy, S.J., Hofmann, M.: Phys. Rev. Lett. **110**, 217211 (2013)
9. Wang, J.L., Campbell, S.J., Studer, A.J., Avdeev, M., Zeng, R., Dou, S.X.: J. Phys. Condens. Matter **21**, 124217 (2009)
10. Md Din, M.F., Wang, J.L., Campbell, S.J., Zeng, R., Hutchison, W.D., Avdeev, M., Kennedy, S.J., Dou, S.X.: J. Phys. D Appl. Phys. **46**, 445002 (2013)
11. Wang, J.L., Campbell, S.J., Hofmann, M., Kennedy, S.J., Zeng, R., Md Din, M.F., Dou, S.X., Arulraj, A., Stusser, N.: J. Phys. Condens. Matter. **25**, 386003 (2013)
12. Welter, R., Venturini, G., Ressouche, E., Malaman, B.: J. Alloy Compd. **218**, 4 (1995)
13. Kervan, S., Elerman, Y., Acet, M.: J. Alloy Compd. **335**, 70 (2002)
14. Kervan, S., Elerman, Y., Acet, M.: J. Alloy Compd. **321**, 35 (2001)
15. Venturini, G., Welter, R., Ressouche, E., Malaman, B.: J. Alloy Compd. **224**, 262 (1995)
16. Venturini, G.: J. Alloy Compd. **232**, 133 (1996)
17. Norlidah, M.N., Venturini, G., Malaman, B., Ressouche, E.: J. Alloy Compd. **245**, 80 (1996)
18. Norlidah, M.N., Venturini, G., Malaman, B., Ressouche, E.: J. Alloy Compd. **248**, 112 (1997)
19. Venturini, G., Welter, R., Ressouche, E., Malaman, B.: J. Alloy Compd. **223**, 101 (1995)
20. Venturini, G., Welter, R., Ressouche, E., Malaman, B.: J. Magn. Magn. Mater. **150**, 197 (1995)
21. Kumar, P., Singh, N.K., Suresh, K.G., Nigam, A.K., Malik, S.K.: J. Appl. Phys. **101**, 013908 (2007)
22. Hofmann, M., Campbell, S.J., Knorr, K., Hull, S., Ksenofontov, V.: J. Appl. Phys. **91**, 8126 (2002)
23. Md Din, M.F., Wang, J.L., Campbell, S.J., Studer, A.J., Avdeev, M.: Appl. Phys. Lett. **104**, 042401 (2014)
24. Elmali, A., Dincer, I., Elerman, Y.: J. Alloy Compd. **370**, 31 (2004)
25. Dincer, I., Elmali, A., Elerman, Y.: J. Magn. Magn. Mater. **280**, 44 (2004)
26. Fujiwara, T., Fujii, H., Shigeoka, T.: Phys. B. **281**, 161 (2000)
27. Kervan, S., Elerman, Y., Acet, M.: J. Alloy Compd. **321**, 35 (2001)
28. Kumar, P., Singh, N.K., Suresh, K.G.: J. Phys. Condens. Matter. **19**, 337 (2007)
29. Wang, J.L., Campbell, S.J., Din, M.F.M.: Phys. Status Solidi **211**, 1092 (2014)
30. Chen, Y.Q., Luo, J., Liang, J.K., Li, J.B., Rao, G.H.: J. Magn. Magn. Mater. **489**, 13 (2010)
31. Kervan, S., Kervan, N., Öztürk, A., Nane, O.: Solid State Commun. **151**, 408 (2011)
32. Brabers, J.H.V.J., Bakker, K., Nakotte, H., de Boer, F.R., Lenczowski, S.K.J., Buschow, K.H.J.: J. Alloy Compd. **199**, L1 (1993)
33. van Dover, R.B., Gyorgy, E.M., Cava, R.J., Krajewski, J.J., Felder, R.J., Peck, W.F.: Phys. Rev. B. **47**, 6134 (1993)
34. Fujii, H., Okamoto, T., Shigeoka, T., Iwata, N.: Solid State Commun. **53**, 715 (1985)
35. Inoue, J., Shimizu, M.: J. Phys. F. Met. Phys. **12**, 1811 (1982)
36. Liu, X.B., Altounian, Z.: J. Magn. Magn. Mater. **292**, 83 (2005)
37. Duc, N.H., Kim Anh, D.T., Brommer, P.E.: Phys. B. **319**, 1 (2002)
38. FÖldeàki, M., Chahine, R., Bose, T.K.: J. Appl. Phys. **77**, 3528 (1995)